IEEE Access
Multidisciplinary | Rapid Review | Open Access Journal

Received April 17, 2017, accepted May 7, 2017, date of publication May 18, 2017, date of current version June 28, 2017.

Digital Object Identifier 10.1109/ACCESS.2017.2705739

Switchable Long-Term Evolution/ Wireless Wide Area Network/ Wireless Local Area Network Multiple-Input and Multiple-Output Antenna System for Laptop Computers

SHU-CHUAN CHEN, (Member, IEEE), AND CHEN-SHUO FU
Department of Electrical and Electronic Engineering, CCIT, National Defense University, Taoyuan 335, Taiwan
Corresponding author: Shu-Chuan Chen (chensc@ema.ee.nsysu.edu.tw)

ABSTRACT This paper introduces a multiple-input and multiple-output (MIMO) antenna system for deployment in the closed hinge slot region of notebook computers for long-term evolution (LTE)/wireless wide area network (WWAN)/wireless local area network (WLAN) applications. This antenna system was placed in the closed hinge slot region formed by the full metal cover, metal ground plate, and metal hinges. The MIMO antenna system, includes a main antenna (Ant 1), an auxiliary antenna (Ant 2), and an isolation element. The main and auxiliary antennas were integrated with the metal surrounding them and were used to excite several resonance modes of the closed hinge slot. Excellent antenna efficiency was achieved using the small antennas. Although Ant1 and Ant2 are only 25 mm $\times$ 5 mm in size, they could cover LTE/WWAN or WLAN operating bands by switching feed points in the same antenna pattern. The isolation element—a 10 mm $\times$ 6 mm metal sheet—was placed at the center of the closed hinge slot region, and enhanced isolation by more than 7 dB. The isolation levels exceeded 18 dB for LTE700/2300/2500 bands and 15 dB for 2.4/5.2/5.8 GHz WLAN bands.

INDEX TERMS Computer antennas, MIMO antennas, LTE/WWAN antennas, WLAN antennas.

I. INTRODUCTION

As the wireless industry grows and high-technology products evolve continually, consumers are demanding higher visual appeal in their mobile communication devices. In addition to larger displays, which can be achieved by adopting narrow-bezel designs, consumers are expecting devices with superior strength and style. Therefore, all-metal chassis and narrow-bezel designs have become a current design trend, resulting in limited space being available for device aerials. Moreover, the bandwidth and efficiency of an antenna are influenced by its installation space and surrounding metal elements. Developing an antenna design technology that effectively integrates the metal environment is thus crucial. With the development of fourth-generation (4G) mobile communication technology [i.e., long-term evolution (LTE)], multiple-input and multiple-output (MIMO) antenna systems have become essential for fast signal transmission. Thus, the current challenges are arranging LTE and wireless local area network (WLAN) MIMO antenna systems within the limited space of mobile communication devices, ensuring sufficient isolation between antennas, and maintaining excellent communication quality.

In numerous studies, miniaturized antennas have been applied to mobile communication devices with narrow bezels [1]–[4]. In these studies, different matching circuits have been used for parallel chip capacitors and inductors to enhance bandwidth and minimize antenna size. Although antenna profiles can be shrunk to 8 mm to meet the narrow-border design requirements, such antennas cannot be used in notebook computers with full metal covers. Recently, some antennas have been designed for devices with metal covers, such as tablet computers and handsets [5]–[10]. Many of these antennas are slot antennas that can easily integrate with the metal environment [5]–[8]. Some of them use high- and low-pass matching circuits to enhance bandwidth [5]–[7], whereas others use a metal ring frame [8]. Although these antennas can be used in metal covers, nonmetal regions are required for slot paths. Some antennas are arranged in the closed hinge slots of notebook computers [9]–[15]; these antennas can be deployed in notebook computers with full

metal covers and narrow bezels. In a previous implementation of such a design [10], a 71.5 mm × 6.5 mm × 3.5 mm antenna was required to cover the LTE and WWAN operating bands. However, the antenna efficiency was unsatisfactory because it was surrounded by ground metal planes. In [11]–[13], the closed hinge slot of a notebook computer was integrated as part of the antenna design. This design not only excited the resonance modes of the antenna but also induced the resonance modes of the closed hinge slot, effectively minimizing the space requirement of the antenna and displaying excellent radiation efficiency. However, the required profile of the antenna was 8 mm, and the antenna could not support a MIMO transmission system. Furthermore, the antenna reported in [14] is unsuitable for conventional slim laptops with metal covers because it requires several grounding and feeding metallic strips across the gap between the display and the keyboard grounds, which limits the feasible arrangement positions of the hinges.

In this paper, we present a MIMO antenna system for thin laptop computers with full metal covers. We set the hinge height at 6 mm and propose an LTE/WWAN/WLAN MIMO antenna system in the closed hinge slot region of laptop computers. The main and auxiliary antennas are arranged in the closed hinge slot. Both the main and auxiliary antennas are 25 mm × 5 mm in size. If two feed positions are used, the LTE/WWAN (LET700/GSM850/900/GSM1800/1900 / UMTS /LTE2300/2500) or WLAN (2.4/5.2/5.8 GHz WLAN) operating bands can be switched under an identical antenna structure. A 10 mm × 6 mm metal-sheet isolation element is placed at the central region of the closed hinge slot to improve the isolation between the main and auxiliary antennas. In the experiments, the isolation in the LTE700/2300/2500 bands exceeded 18 dB, and the isolation in 2.4/5.2/5.8 GHz WLAN bands exceeded 15 dB. The antenna design and measurement results are detailed in Section II. In Section III, compatibility is explored, and in Section IV, the conclusions are summarized.

II. PROPOSED MIMO ANTENNA DESIGN

A. MIMO ANTENNA SYSTEM

Fig. 1(a) presents the geometry of the MIMO antenna system, which consists of a main antenna, an auxiliary antenna, and an isolation element. The size of the full metal cover and the metal ground plane is 310 mm × 200 mm, which is suitable for a 14-inch laptop computer. The main and auxiliary antennas have the same structure [Fig. 1(c)] and are arranged back-to-back in the closed hinge slot region; each is at a distance of 15 mm from the right or left metal hinge. The isolation element, a metal sheet measuring 10 mm × 6 mm, is placed at the central region of the closed hinge slot, 140 mm from the left and right metal hinges [Fig. 1(b)]. The isolating element separates the main and auxiliary antennas into two closed hinge slots, Slot 1 and Slot 2, to reduce the coupling between the antennas. The size of the two short closed hinge slots is 140 mm × 6 mm.

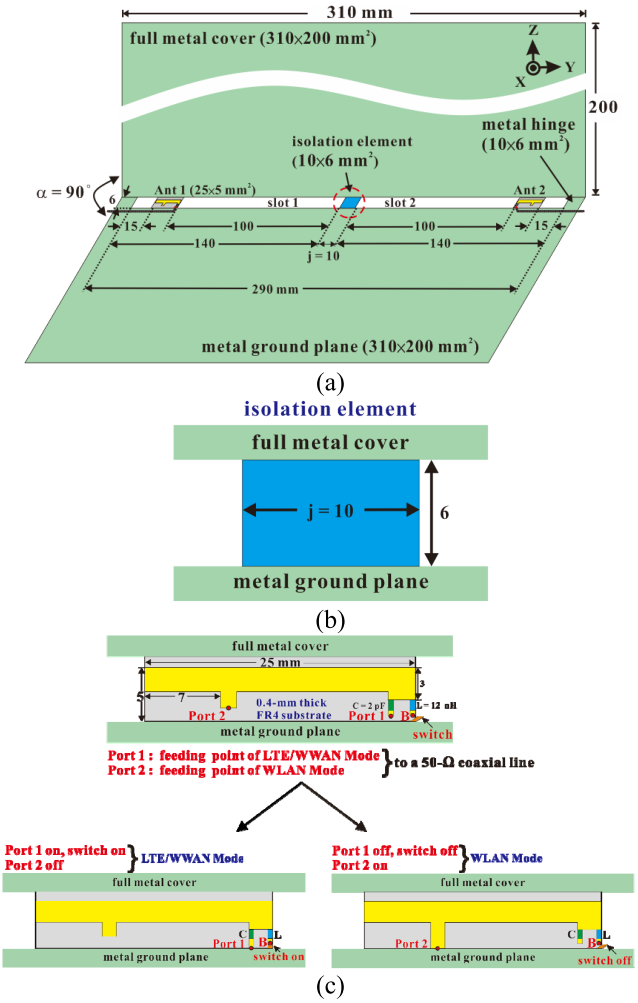

FIGURE 1. Geometry of (a) the proposed MIMO antenna system, (b) the isolation element, and (c) the main antenna.

For physical experiments, the main antenna was printed on a 0.4-mm-thick FR4 substrate of size 25 mm × 6 mm. It comprised a metal strip, a chip capacitor, a chip inductor, and a switch element within a 25 mm × 5 mm area. A 1-mm gap was set between the metal strip and the full metal cover to excite the resonance modes of the short closed hinge slot (Slot 1) in order to enhance the operating bandwidth of the antenna. Port 1 served as the signal feed point of the LTE/WWAN antenna and was connected to the internal conductor of a 50-Ω mini coaxial line. Port 2 served as the signal feed point of the WLAN antenna and was also connected to the internal conductor of the 50-Ω mini coaxial line. Port 1 was connected to a 2-pF series chip capacitor, which was in turn connected to a metal strip. A 12-nH chip inductor was connected to a metal strip and to Point B, 2 mm from the chip capacitor, which was in turn connected to a switch element. The switch element was used to determine whether to connect to the ground. This metal strip was approximately 25 mm × 2.2 mm. Port 2 was placed 7.5 mm from the left opening of the metal strip. When Port 1 was fed and the switch element was connected to Point B, the main antenna

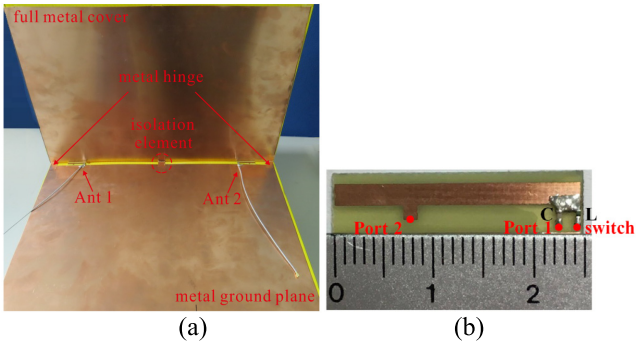

FIGURE 2. Prototype of the (a) proposed MIMO antenna system and (b) main antenna.

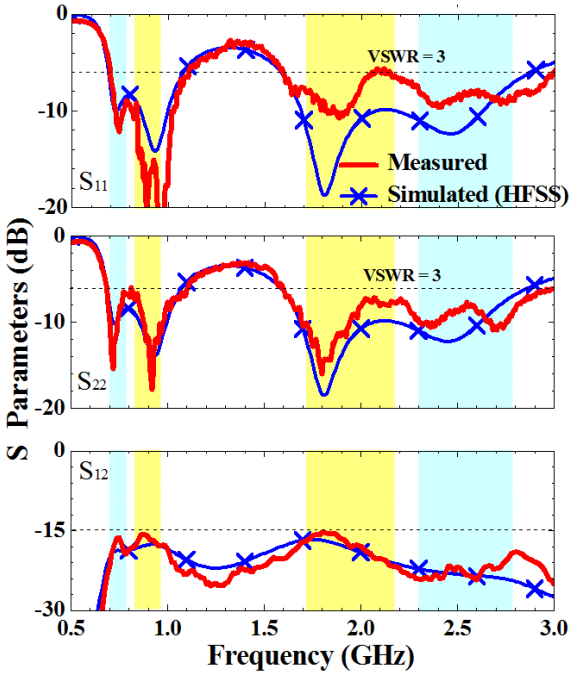

FIGURE 3. Measured and simulated S parameters for the proposed MIMO antenna system in LTE/WWAN bands.

formed a planar inverted-F antenna (PIFA), which excited several resonance modes of the PIFA and Slot 1 to cover the required LTE/WWAN bands. When Port 2 was fed and the switch was not connected to Point B, the main antenna formed a T-shaped monopole structure, which excited several resonance modes of the monopole antenna and Slot 1 to cover the 2.4/5.2/5.8 GHz WLAN bands.

B. EXPERIMENT AND MEASUREMENT RESULTS

Fig. 2(a) and Fig. 2(b) illustrate the prototype of the proposed MIMO antenna system and the main antenna. Fig. 3 and Fig. 4 show the measured and simulated S parameters in the proposed MIMO antenna system in the LTE/WWAN and WLAN bands. Simulated results were obtained using the ANSYS HFSS version 15 (full-wave electromagnetic field simulator) [16]. The measured and simulated S parameters for the proposed MIMO antenna system in LTE/WWAN band are depicted in Fig. 3. When Port 1 was in operation, the main and

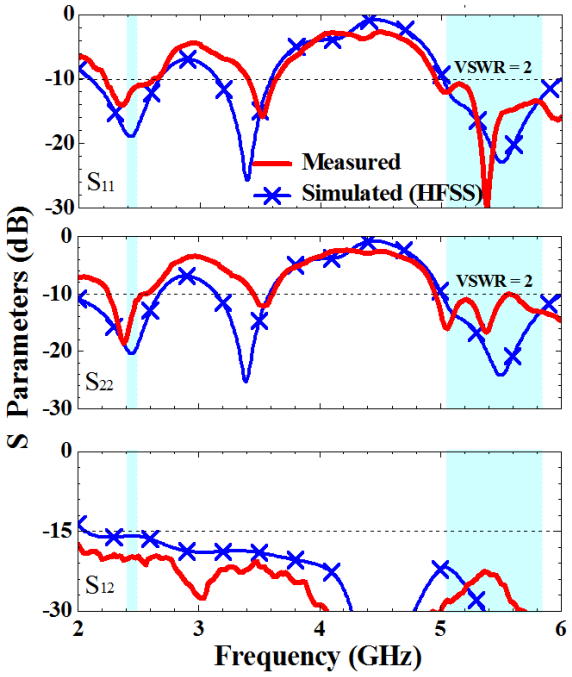

FIGURE 4. Measured and simulated S parameters for the proposed MIMO antenna system in WLAN bands.

auxiliary antennas could cover low-band (698–960 MHz) and high-band operations (1710–2690 MHz), thus meeting the requirements of the LTE/WWAN bands (LTE700/GSM850 /900/GSM1800/1900/UMTS/LTE2300/2500). Regarding impedance bandwidth, the return loss standard was higher than 6 dB (i.e., voltage standing wave ratio (VSWR) = 3:1). The isolation levels in the LTE and WLAN bands were higher than 18 and 16 dB, respectively. The measured and simulated S parameters for the proposed MIMO antenna system in WLAN bands are shown in Fig. 4. When Port 2 was in operation, the main and auxiliary antennas could cover the 2.4/5.2/5.8 GHz WLAN bands. Regarding the impedance bandwidth, the return loss standard was higher than 10 dB (i.e., VSWR = 2:1). The isolation levels in the 2.4-GHz WLAN and 5.2/5.8-GHz WLAN band were higher than 15 and 23 dB, respectively.

For MIMO antenna systems, envelope correlation coefficients (ECCs) less than 0.5 are practical [17]. Measured and simulated ECCs for the LTE/WWAN and WLAN antenna systems are shown in Fig. 5 and Fig. 6, respectively. The measured ECC was computed from the radiation-pattern-based formula [18] given as

$$\rho_{e,ij} = \left| \frac{\iint_{\Omega} \left(E_{\theta,i} E^*_{\theta,j} + E_{\varphi,i} E^*_{\varphi,j} \right) d\Omega}{\sqrt{\iint_{\Omega} \left(|E_{\theta,i}|^2 + |E_{\varphi,i}|^2 \, d\Omega \right) \iint_{\Omega} \left(|E_{\theta,i}|^2 + |E_{\varphi,i}|^2 \, d\Omega \right)}} \right| \quad (1)$$

It can be seen that the measured ECCs is higher than those in the simulation. The corresponding measured ECCs in the

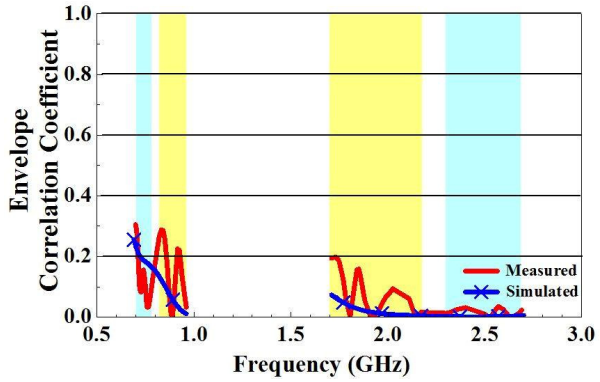

FIGURE 5. Measured and simulated ECCs for the LTE/WWAN antenna system.

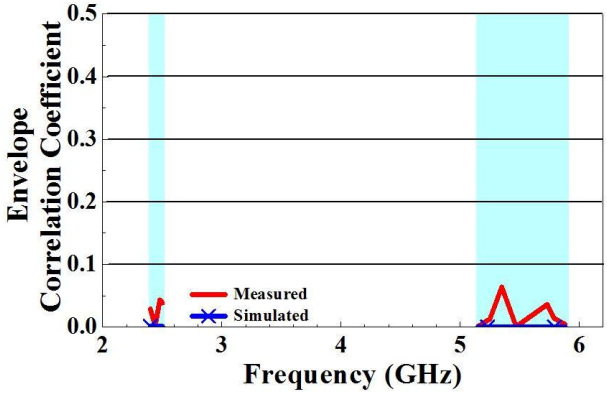

FIGURE 6. Measured and simulated ECCs for the WLAN antenna system.

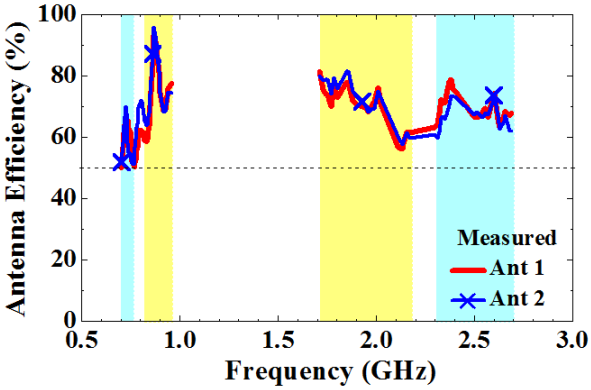

FIGURE 7. Measured antenna efficiency of the main and auxiliary antennas in the LTE/WWAN band.

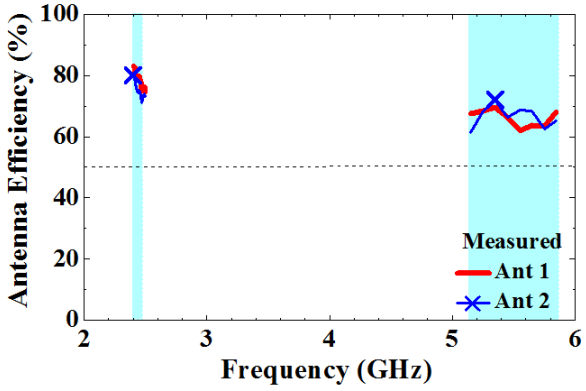

FIGURE 8. Measured antenna efficiency of the main and auxiliary antennas in the WLAN band.

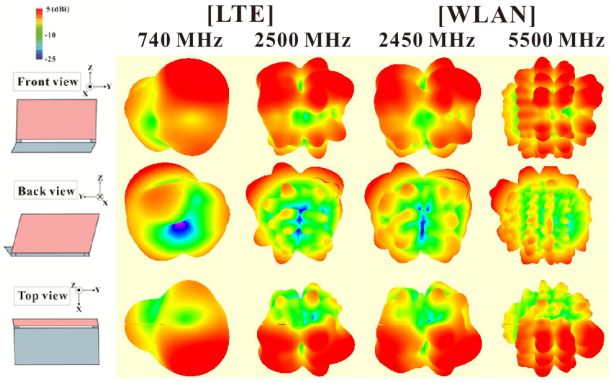

FIGURE 9. Measured 3D radiation patterns of the main antenna (Ant 1) in the LTE and WLAN bands.

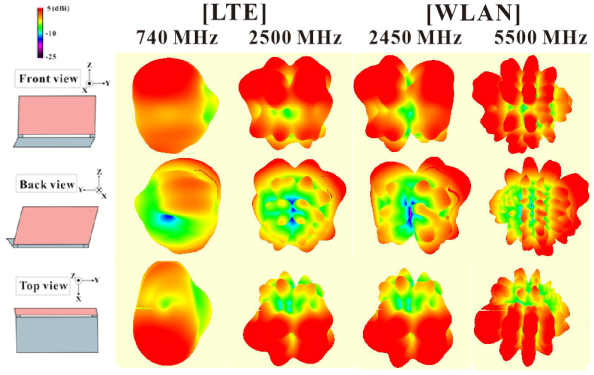

FIGURE 10. Measured 3D radiation patterns of the auxiliary antenna (Ant 2) in the LTE and WLAN bands.

LTE/WWAN and WLAN system are less than 0.31 and 0.07, respectively, all of which are less than the ECC criterion of 0.5. It can also be seen that the measured and simulated curves with some errors that may be caused by the material parameters hypothesis, implementation process, measurement environment, etc.

Fig. 7 shows the measured antenna efficiency when the proposed MIMO antenna system operated in the LTE/WWAN bands. The antenna efficiencies of the main and auxiliary antennas were approximately 50%–93% in the low band and approximately 56%–81% in the high-band. Fig. 8 shows the measured antenna efficiency when the proposed MIMO antenna system operated in the WLAN band. The antenna efficiencies of the main and auxiliary antennas were approximately 74%–83% in the low band and approximately 63%–69% in the high band.

The measured 3D radiation patterns of the main antenna (Ant 1) at 740 and 2500 MHz for LTE bands and

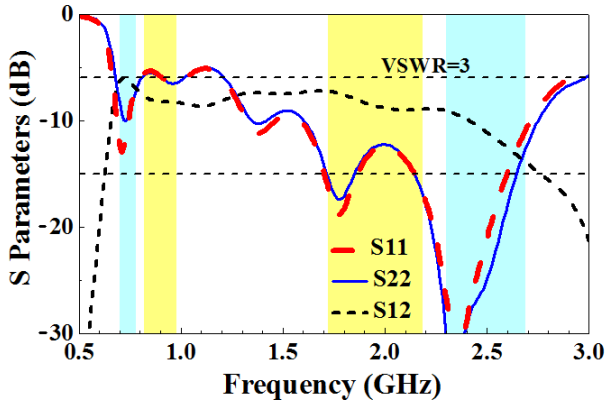

FIGURE 11. Simulated S parameters for the proposed MIMO antenna system without the isolation element in LTE/WWAN operation.

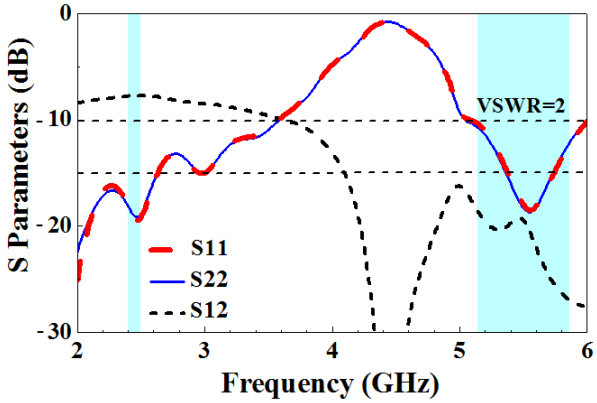

FIGURE 12. Simulated S parameters for the proposed MIMO antenna system without the isolation element in WLAN operation.

2450 and 5500 MHz for WLAN bands are shown in Fig. 9, and the measured 3D radiation patterns of the auxiliary antenna (Ant 2) at these frequencies, which are the center frequencies of the low and high bands of the LTE/WLAN bands, respectively, are shown in Fig. 10. The radiation pattern at 740 MHz is smoother than those at 2450, 2500, and 5500 MHz; this was due to the numerous current nulls at high frequencies. When the main antenna (Ant 1) was in operation, the radiation was stronger in the left radiation pattern of the main antenna (and in the direction of $-$y), and when the auxiliary antenna (Ant 2) was in operation, the radiation was stronger in the right radiation pattern of the auxiliary antenna (and in the direction of $+$y). Thus, radiation intensity is related to antenna position.

C. DESIGN OF THE MIMO ANTENNA SYSTEM

To further clarify the effect of isolation, the isolation of the proposed MIMO antenna system without the isolation element was analyzed. According to the reciprocity theorem, the reception and radiation characteristics of antennas are identical. Thus, S_{21} equals S_{12}. In the present design, S_{21} denotes the isolation of MIMO antennas ($-20\log_{10}|S_{21}|$). Fig. 11 and Fig. 12 present the simulation diagrams of S parameters for the proposed MIMO antenna system without the isolation element in the LTE/WWAN and WLAN band, respectively. As shown in these figures, the isolation in the LTE700 and GSM850/900 bands were 6–7 and 7–8 dB, respectively. In the GSM1800/1900/UMTS and LTE2300/2500 bands, the isolation was about 7–9 and 9–14 dB, respectively. In the 2.4 GHz WLAN band, the isolation was 7–8 dB. In the 5.2/5.8 GHz WLAN bands, the isolation was about 18–26 dB. Apart from the 5.2/5.8 GHz WLAN bands, the isolation in the other bands were less than 15 dB. Fig. 3 and Fig. 4 show the measured and simulated S parameters for the proposed MIMO antenna system (with the isolation element) in LTE/WWAN and WLAN operation, respectively.

We compared the isolation with (in Fig. 3 and Fig. 4) and without (in Fig. 11 and Fig. 12) isolation elements. With the addition of the isolation element, the isolation in the LTE 700 band improved by approximately 11 dB to more than 18 dB. The isolation in the LTE2300/2500 bands was improved about 13 dB to more than 22 dB. The isolation in the GSM850/900 bands was improved 10 dB to more than 17 dB. The isolation in the GSM1800/1900/UMTS bands was improved about 9 dB to more than 16 dB. The isolation in the 2.4 GHz WLAN band was improved about 7 dB to more than 15 dB. The isolation in the 5.2/5.8 GHz WLAN bands was improved about 5 dB to more than 23 dB.

The improvement in the isolation can be explained as follows. Without an isolation element, several resonance modes of the main and auxiliary antennas were contributed by the long closed hinge slot [11]–[13]. Therefore, the mutual coupling between the two antennas was serious and the isolation was thus poor. With the addition of the isolation element, the long closed hinge slot was divided into two short closed hinge slots at the right- and left-hand sides (Slots 1 and 2). Therefore, the resonance modes of Slots 1 and 2 were excited to substitute for the resonance modes of the long closed hinge slot, which effectively reduced the coupling between the two antennas and improved the isolation in the LTE/WWAN/WLAN bands. To further verify the performance of the isolation element, the ground plane current and the electrical field distributions for the proposed MIMO antenna system with and without the isolation element were analyzed.

The design of the main antenna was identical to that of the auxiliary antenna. Thus, we only show the current and electric-field distributions for the main antenna (Ant1) in operation. Fig. 13 shows comparisons of the simulated ground current distribution for the proposed MIMO antenna system with and without the isolation element at 742 and 2500 MHz for LTE operation. Fig. 14 shows comparisons of the simulated ground current distribution for the proposed MIMO antenna system with and without the isolation element at 2450 and 5550 MHz for WLAN operation. The isolation element substantially reduced the lateral ground current from the main antenna to the auxiliary antenna

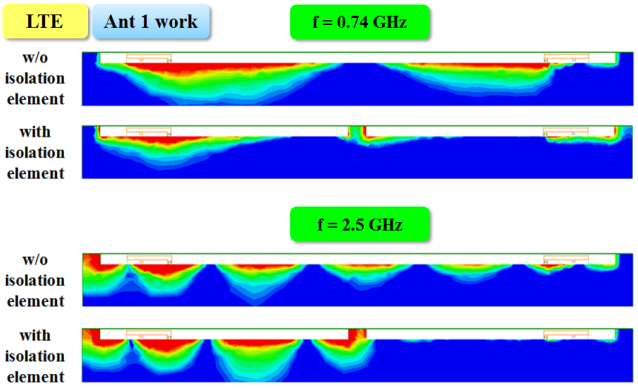

FIGURE 13. Simulated ground current distribution for the proposed MIMO antenna system with and without the isolation element at 742 and 2500 MHz for LTE operation.

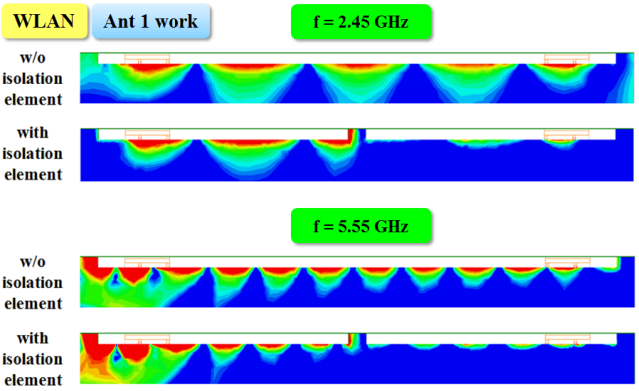

FIGURE 14. Simulated ground current distribution for the proposed MIMO antenna system with and without the isolation element at 2450 and 5550 MHz for WLAN operation.

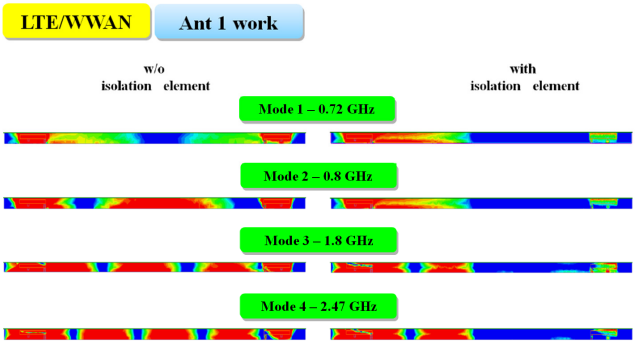

FIGURE 15. Simulated electric-field distribution in the closed hinge slot region with and without an isolation structure at 720, 800, 1800, and 2470 MHz for LTE/WWAN operation.

and improved the isolation between the two antennas. The improvement level of ground current distribution for WLAN band is not as good as in the LTE band. Because the isolation in LTE/WWAN band was improved about 10 dB, but in WLAN band was only about 5 dB.

In addition, to determine whether the isolation element changed the resonance path of the closed hinge slot, the electric-field distributions in the closed slot at the main antenna (Ant 1) were analyzed. Fig. 15 shows comparisons

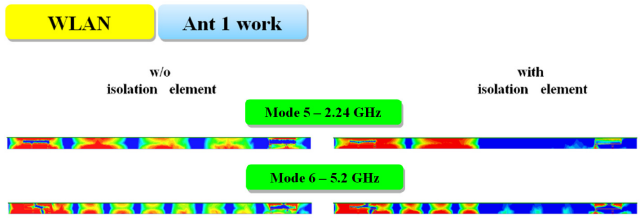

FIGURE 16. Simulated electric-field distribution in the closed hinge slot region with and without an isolation structure at 2240 and 5200 MHz (Mode 5 and Mode 6) for WLAN operation.

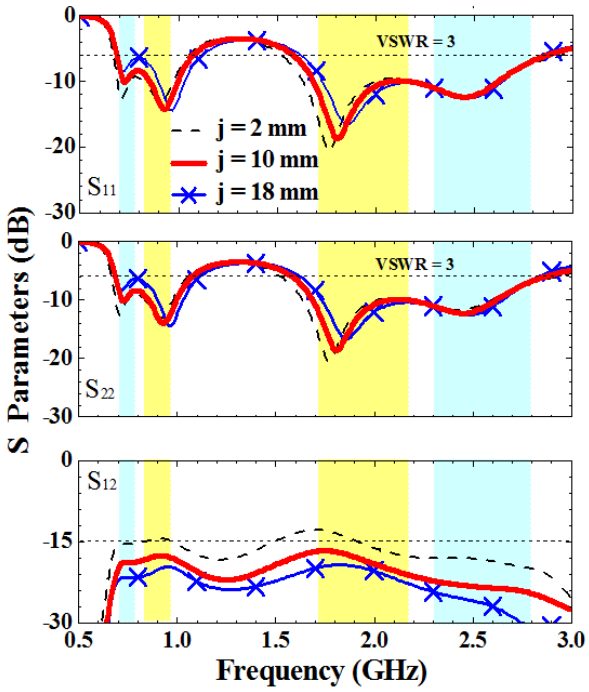

FIGURE 17. Simulated S parameters for the proposed MIMO antenna system as a function of the width j of the isolation structure in LTE/WWAN operation.

of the simulated electric-field distribution in the closed hinge slot region with and without the isolation structure at 720, 800, 1800, and 2470 MHz (Mode 1, Mode 2, Mode 3, and Mode 4, respectively) for LTE/WWAN operation. Fig. 16 shows comparisons of the simulated electric-field distribution in the closed hinge slot region with and without the isolation structure at 2240 and 5200 MHz (Mode 5 and Mode 6, respectively) for WLAN operation. In the absence of the isolation element, the resonance modes of the long closed hinge slot were excited by the main antenna (Ant 1). However, in the presence of the isolation element, the resonance modes of the short closed slot (Slot 1) were excited by the main antenna (Ant 1). Therefore, the isolation between the main and auxiliary antennas was improved.

III. PARAMETRIC ANALYSIS

Fig. 17 and Fig. 18 show the simulated S parameters for the proposed MIMO antenna system as a function of the width j in the isolation structure in LTE/WWAN and WLAN

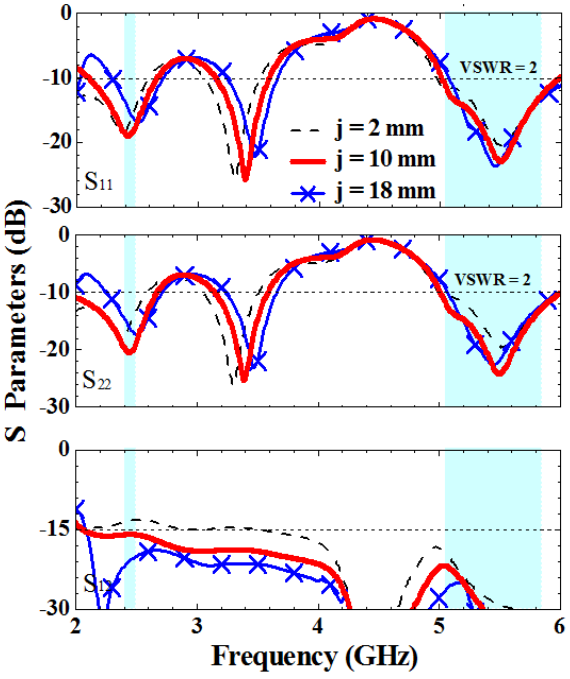

FIGURE 18. Simulated S parameters for the proposed MIMO antenna system as a function of the width j of the isolation structure in WLAN operation.

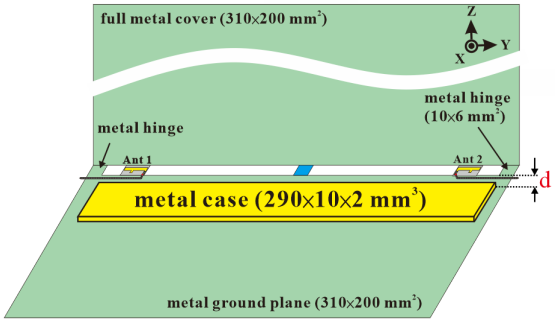

FIGURE 19. Schematic of the proposed MIMO antenna system integrated with its metal case.

operation, respectively; the width was increased by the same amount on the left and right side. When the width of the isolation structure was increased from 2 to 18 mm, no noteworthy change was observed in the S_{11} and S_{22} curves. However, a simulated isolation structure with increased width improved the isolation, because the increase in the width of the isolation structure could more effectively isolate the electric field in the two short closed slots (Slot 1 and Slot 2), in turn improving the isolation between the main and auxiliary antennas. We advocate a width of 10 mm rather than 18 mm because an excessively wide isolation structure produces an unsightly device.

IV. COMPATIBILITY OF THE PROPOSED MIMO ANTENNA SYSTEM

For the present design (Fig. 19), the compatibility of the proposed MIMO antenna system with peripheral metal

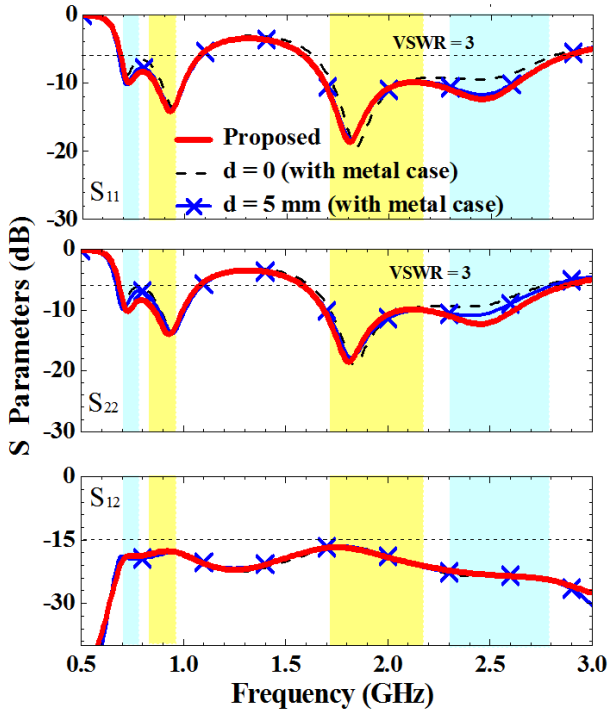

FIGURE 20. Simulated S parameters for the proposed MIMO antenna system and its integrated metal case in LTE/WWAN operation.

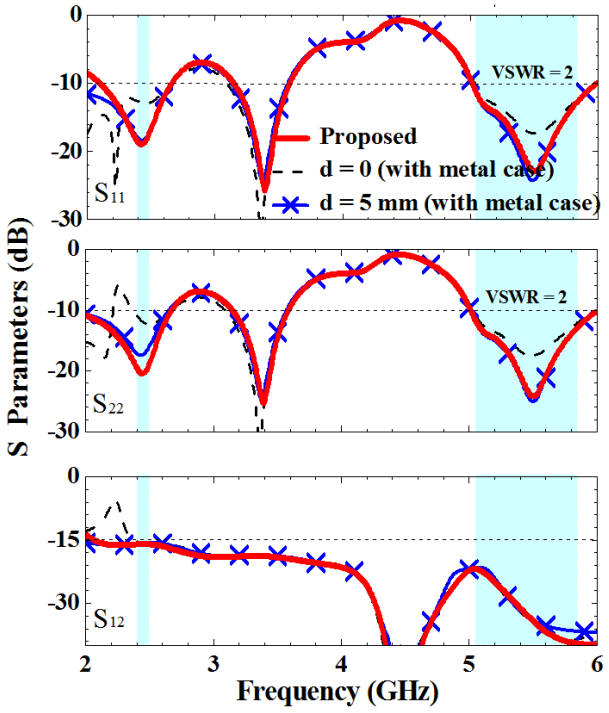

FIGURE 21. Simulated S parameters for the proposed MIMO antenna system and its integrated metal case in WLAN operation.

components was analyzed. In this analysis, the size of the metal case was 290 mm × 10 mm × 2 mm, and the length of the metal case was identical to the length of the closed hinge slot. Fig. 20 and Fig. 21 show the simulated S parameters

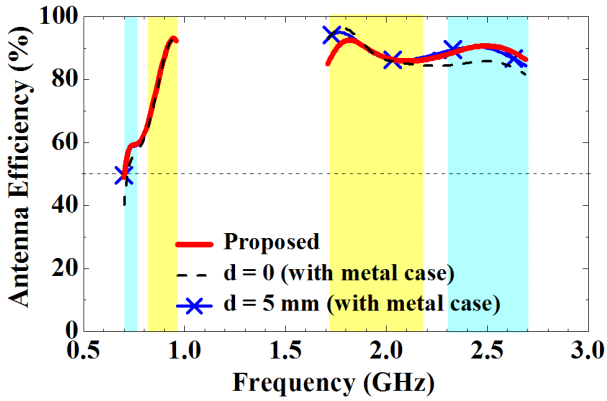

FIGURE 22. Simulated antenna efficiencies for the proposed MIMO antenna system and its integrated metal case in LTE/WWAN operation.

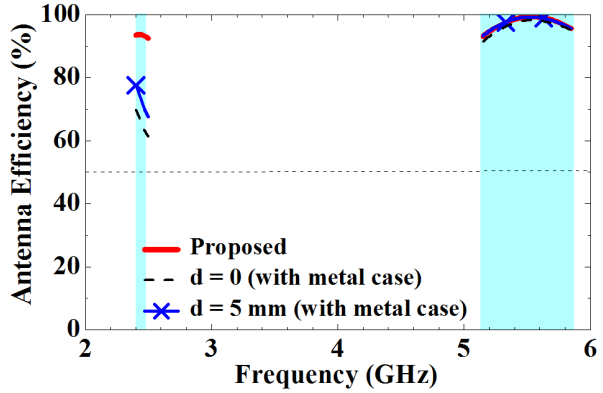

FIGURE 23. Simulated antenna efficiencies for the proposed MIMO antenna system and its integrated metal case in WLAN operation.

for the proposed MIMO antenna system and its integrated metal case at 0 and 5 mm below the closed hinge slot in LTE/WWAN and WLAN operation, respectively. Clearly, S_{11} and S_{22} for the integration with the metal case could still cover the required operating bands. In addition, S_{12} was less than -15 dB in LTE/WWAN and WLAN operation. It can be seen that the proposed MIMO antenna system and metal components have good compatibility.

Fig. 22 and Fig. 23 show the simulated antenna efficiencies for the proposed MIMO antenna system and its integrated metal case at 0 and 5 mm below the closed hinge slot in LTE/WWAN and WLAN operation, respectively. Clearly, the efficiencies in the LTE700 band were reduced to approximately 40%, and the efficiencies in the other operating bands remained higher than 50%. Therefore, the proposed MIMO antenna system could be integrated with peripheral metal components with acceptable antenna characteristics.

V. CONCLUSION

This study proposed an LTE/WWAN/WLAN MIMO antenna system for laptop computers. The closed hinge slot was integrated into a part of the antenna, which made the antenna with small size have good antenna efficiency. In addition, by designing two feed points and a switch element in the main and auxiliary antennas, the antennas could cover either the LTE/WWAN or WLAN bands. The measured antenna efficiencies in the LTE/WWAN/WLAN bands were more than 50%. This study also proposed a simple isolation structure design to enhance the isolation between the main and auxiliary antennas. The isolation in the LTE and WLAN operating bands were more than 15 dB. This design is compatible with peripheral metal components and can thus be applied to laptop computers with all-metal chassis.

REFERENCES

[1] S. C. Chen and K. L. Wong, "Planar strip monopole with a chip-capacitor-loaded loop radiating feed for LTE/WWAN slim mobile phone application," *Microw. Opt. Technol. Lett.*, vol. 53, no. 4, pp. 952–958, Apr. 2011.
[2] K.-L. Wong and L.-Y. Chen, "Small-size LTE/WWAN tablet device antenna with two hybrid feeds," *IEEE Trans. Antennas Propag.*, vol. 62, no. 6, pp. 2926–2934, Jun. 2014.
[3] K. L. Wong and Z. G. Liao, "Small-size dual-wideband monopole antenna with inductive and capacitive feeding branches for long term evolution tablet computer application," *Microw. Opt. Technol. Lett.*, vol. 57, no. 4, pp. 853–860, Apr. 2015.
[4] K. L. Wong and M. T. Chen, "Very-low-profile dual-wideband loop antenna for LTE tablet computer," *Microw. Opt. Technol. Lett.*, vol. 57, no. 1, pp. 141–146, Jan. 2015.
[5] K. L. Wong and P. R. Wu, "Low-profile dual-wideband dual-inverted-L open-slot antenna for the LTE/WWAN tablet device," *Microw. Opt. Technol. Lett.*, vol. 57, no. 8, pp. 1813–1818, Aug. 2015.
[6] K. L. Wong and C. Y. Tsai, "Dual-wideband U-shape open-slot antenna for the LTE metal framed tablet computer," *Microw. Opt. Technol. Lett.*, vol. 57, no. 11, pp. 2677–2683, Nov. 2015.
[7] K. L. Wong and Y. J. Li, "Low-profile open-slot antenna with three Banch slots for triple-wideband LTE operation in the metal-framed smartphone," *Microw. Opt. Technol. Lett.*, vol. 57, no. 10, pp. 2231–2238, Oct. 2015.
[8] C. K. Hsu and S. J. Chung, "Compact multiband antenna for handsets with a conducting edge," *IEEE Trans. Antennas Propag.*, vol. 63, no. 11, pp. 5102–5107, Nov. 2015.
[9] L. Y. Chen and K. L. Wong, "2.4/5.2/5.8 GHz WLAN antenna for the ultra-book computer with metal housing," presented at the APMC, Kaohsiung, Taiwan, Dec. 2012.
[10] S. H. Chang and W. J. Liao, "A compact 3D antenna with comprehensive LTE band coverage for use on notebook hinge," presented at the IEEE Asia–Pacific Conf. Antennas Propag., Singapore, Aug. 2012.
[11] S. C. Chen and Y. C. Tsou, "Small-size LTE/WWAN two-strip monopole exciter antenna integration with metal covers," *IEEE Trans. Antennas Propag.*, vol. 64, no. 8, pp. 3707–3711, Aug. 2016.
[12] S. C. Chen and Y. C. Tsou, "Long-term evolution/wireless wide area network monopole exciter antenna for slim laptop with full metal cover," *Electron. Lett.*, vol. 52, no. 10, pp. 794–796, May 2016.
[13] S. C. Chen and Y. C. Tsou, "Bandwidth enhancement of a monopole exciter by using a chip-inductor-loaded shorted strip," *J. Electromagn. Waves Appl.*, vol. 30, no. 11, pp. 1481–1492, Jul. 2016.
[14] S. Cheng, P. Lindberg, A. Kaikkonen, and P. Hallbjörner, "Internal multiple-input, multiple-output antenna arrays for wireless wide area network and wireless local area network operation in seamless full metal cover laptops," *IET Microw. Antennas Propag.*, vol. 8, pp. 73–79, Jan. 2014.
[15] W. Y. Li, W. J. Chen, and C. Y. Wu, "Multiband 4-port MIMO antenna system for LTE700/2300/2500 operation in the laptop computer," presented at the Asia–Pacific Microw. Conf. (APMC), Kaohsiung, Taiwan, Dec. 2012.
[16] (Mar. 2017). *ANSYS HFSS*. [Online]. Available: http://www.ansys.com/Products/Electronics/ANSYS-HFSS
[17] R. G. Vaughan and J. B. Anderson, "Antenna diversity in mobileommunications," *IEEE Trans. Antennas Propag.*, vol. 36, no. 4, pp. 149–172, Nov. 1987.
[18] D. Sarkar, K. Saurav, and K. V. Srivastava, "A compact dual band four element MIMO antenna for pattern diversity applications," presented at the IEEE 5th Asia–Pacific Conf. Antennas Propag. (APCAP) (APMC), Kaohsiung, Taiwan, Jul. 2016.

SHU-CHUAN CHEN (M'13) received the B.S. and M.S. degrees in electrical engineering from the Chung-Cheng Institute of Technology, National Defense University, Taoyuan, Taiwan, in 1998 and 2004, respectively, and the Ph.D. degree in electrical engineering from National Sun Yat-sen University, Kaohsiung, Taiwan, in 2012. Since 2012, she has been an Assistant Professor with the Department of Electrical and Electronic Engineering, Chung Cheng Institute of Technology, National Defense University, where she became an Associate Professor in 2016. She holds over 20 patents, including U.S., Taiwan, and China patents. Her main research interests are in internal antennas for mobile communication devices.

CHEN-SHUO FU received the B.S. degree in communications engineering from Feng Chia University, Taichung, Taiwan, in 2014, and the M.S. degree in electrical engineering from the Chung-Cheng Institute of Technology, National Defense University, Taoyuan, Taiwan, in 2016.